R. & M. No. 3743

R. & M. No. 3743

LIBRARY
ROYAL AIRCRAFT ESTABLISHMENT
BEDFORD.

PROCUREMENT EXECUTIVE MINISTRY OF DEFENCE

AERONAUTICAL RESEARCH COUNCIL
REPORTS AND MEMORANDA

Some Calculations for Air Resonance of a Helicopter with Non-Articulated Rotor Blades

By J. C. A. BALDOCK
Structures Dept., R.A.E., Farnborough

LONDON: HER MAJESTY'S STATIONERY OFFICE
1974
PRICE £1·20 NET

Some Calculations for Air Resonance of a Helicopter with Non-Articulated Rotor Blades

By J. C. A. Baldock

Structures Dept., R.A.E., Farnborough

Reports and Memoranda No. 3743*

April, 1972

Summary

This Report describes an analysis of air resonance in the hover, and the solutions obtained for a helicopter with non-articulated blades. It is shown that stability in air resonance depends critically on blade structural and aerodynamic parameters that are not easily estimated with the required accuracy, and that a calculation technique requires careful, positive correlation with experiment before its accuracy can be accepted.

The effectiveness of model rotor experiments for checking data is considered, and measurements of rotor impedances show promise of providing a useful basis for comparing with theoretical equivalents.

The effect of an autostabiliser designed to counteract the conventional helicopter instabilities in pitch and roll is investigated. It is found that such an autostabiliser destabilises the air resonance mode.

* Replaces R.A.E. Technical Report 72083—A.R.C. 34 332.

LIST OF CONTENTS

1. Introduction

The 'air resonance' phenomenon is similar to the 'ground resonance' phenomenon, first studied by Coleman.[1] Coleman showed that instabilities were possible, for a helicopter with articulated blades, due to a coupling between airframe body modes involving horizontal translations of the rotor hub, and lagging deflection of the blades about the lag hinge. The body modes he considered were those of the body against the elastic restraint of the undercarriage with the aircraft on the ground. The term 'air resonance' is used to describe a similar coupling between lagging deflection of the blades and airframe body modes when the aircraft is airborne.

For helicopters with non-articulated blades, the motion in air or ground resonance becomes more complicated owing to the fact that there is now significant elastic coupling between body pitch and roll and blade flapping. As most body modes involving hub horizontal translations also involve body pitch and roll, blade flapping becomes coupled into the motion. Thus the analysis is required to be more complicated than that of Coleman, there being a need to consider modes involving hub horizontal translations, body pitch and roll, blade lagging and blade flapping.

Coleman showed in the ground resonance case that, assuming some damping in the undercarriage, the instability would be suppressed by dampers across the blade lag hinges. The blade flapping that will be coupled into the motion with non-articulated blades is heavily damped by aerodynamic forces, and so one of the possibilities to be investigated with non-articulated blades is whether the aerodynamic damping may eliminate the need for artificial blade-damping.

Other investigations[2,3] dealing with non-articulated rotor systems do not reach the same conclusions about the need for artificial blade-damping. These other investigations dealt with 'soft in-plane' blades, that is with blades with the blade fundamental lagging natural frequency lower than the normal rotor operating speed, and they showed that aircraft fitted with such blades were particularly susceptible to the air-resonance instability. A rotor with 'soft in-plane' blades is taken in this work. The emphasis in the study is on a critical examination of the sensitivities to any lack of precision in the assumptions and input data, rather than on an exhaustive analysis of the air resonance phenomenon. The analysis is restricted to the zero forward speed case.

A helicopter is likely to be fitted with an autostabiliser designed to counteract the conventional helicopter instabilities in pitch and roll in forward flight. A typical autostabiliser would apply cyclic pitch to the blades according to a law including body pitch and roll displacements and velocities. This coupling between the body and the rotor may have an unwanted effect on the air resonance condition, and so its effect is considered.

2. Equations of Motion

2.1. Introduction

The linearised equations of motion are formulated using the 'semi-rigid' representation, in which it is assumed that the continuous system may be represented by a finite number of modes of distortion. These modes are taken as the basis of a system of generalised coordinates in Lagrange's equations of motion. The basic data required to analyse the system are its geometry, mass distribution, and the shapes and frequencies of the assumed modes of deformation of the body and the rotor blades. Articulated or non-articulated blades may be represented simply by appropriate choice of mode shapes and frequencies. In the semi-rigid representation, the choice of the modes of deformation to be included can prove to be fundamental to the accuracy achieved. Consequently the sensitivity of the results to the modes chosen, must be determined as an important part of the investigation.

Given the definition of geometry, mass distribution, displacements in the modes chosen and basic aerodynamic assumptions, Lagrange's equations of motion are derived by a formal, analytic procedure, and a computer programme written[5] to evaluate the expressions. The procedure is fully described in a preliminary note[4] but, for convenience, the basic assumptions and definitions are repeated here.

2.2. Choice of Body Modes

Section 1 indicates that body modes involving hub horizontal translations, pitch and roll are concerned in the phenomenon. In this initial work, the fuselage is assumed to be rigid, and the body modes assumed are:–

(a) rigid body lateral translation,
(b) rigid body fore and aft translation,
(c) rigid body vertical translation,
(d) rigid body roll and
(e) rigid body pitch.

force and the assumption of a constant length of beam during flapping or lagging deflection) require the retention of deflections to order (q^2) in order that correct order (q) equations are obtained. For these terms, the form of deflection in equation (2) has to be extended.

2.3.2. *Modes assumed initially for this work.* The source of the data for the blade modes was a calculation of the blade normal modes using the Holzer–Myklestad transfer matrix method. The equilibrium position of the blade at a standard rotor-rotation speed and collective-pitch setting was found, and from this datum position, the shapes and frequencies of the blade normal modes were found (Coriolis forces were neglected). Each normal mode involved flap bending, lag bending and twist, but modes with predominantly flap bending and predominantly lag bending could be identified. The initial choice of modes for the air resonance work was:

(a) the flap bending part alone from the predominantly flap bending normal mode,

(b) the lag bending part alone from the predominantly lag bending normal mode and

(c) uniform pitch rotation about the reference axis—this was not associated with a deformation coordinate but introduced as a computational device required for the representation of cyclic pitch in the autostabiliser work—*see* Section 3.

2.4. Aerodynamic Assumptions

Simple assumptions were made. Fig. 4 shows a cross-section of the blade, normal to the blade reference axis. Fig. 4 also shows how the lift and drag per unit span of the blade were found from the reference axis velocities v_1 and v_3. The velocities v_1 and v_3 are found in Ref. 4 by a series of axis transformations, various sets of axes being used to define the basic geometry and the distortions allowed (some of these axis sets are shown in Figs. 1–3). A constant and uniform induced flow velocity λ is allowed through the rotor disc. This is assumed to be parallel to the rotor shaft. As an example of the application of the assumptions of Fig. 4, in the steady state in the hover, Ref. 4 gives

$$v_1 = \lambda - r\Omega\alpha_0$$

and

$$v_3 = r\Omega,$$

where r is the distance of the section from the hub,

Ω is the rotor rotation speed,

λ is the induced flow velocity

and α_0 is the collective pitch, defined in Fig. 1.

Thus

$$\bar{L} = -\rho c l_\alpha r^2\Omega^2\left[\left(\frac{\lambda}{r\Omega}\right) - \alpha_0\right]$$

$$\bar{D} = \tfrac{1}{2}\rho c C_D[(r\Omega)^2 + (\lambda - r\Omega\alpha_0)^2].$$

2.5. Use of Coleman Transformations

Section 2.3 describes the definition of the modal deflections for a single blade. When all the blades—of a four-bladed rotor in the case taken here—are considered, it is obvious that similar modes will have to be assumed for each blade, and that the coupling terms with the body modes must include periodic functions describing the position of a blade in azimuth. Coleman[1] shows how, with the terms arising from the mass of the rotating system with three or more blades, the periodic terms may be avoided by the use of transformations. It is found that these transformations are also successful in avoiding periodic terms in the aerodynamic forces at zero forward speed. At finite forward speed, periodic terms remain even after the Coleman transformations, but this case is not considered here.

The Coleman transformations for a four-bladed rotor are:

$$\begin{bmatrix} {}_1q \\ {}_2q \\ {}_3q \\ {}_4q \end{bmatrix} = \begin{bmatrix} I & I\cos\Omega t & 0 & I\sin\Omega t \\ 0 & -I\sin\Omega t & I & I\cos\Omega t \\ I & -I\cos\Omega t & 0 & -I\sin\Omega t \\ 0 & I\sin\Omega t & I & -I\cos\Omega t \end{bmatrix} \begin{bmatrix} q_1^* \\ q_2^* \\ q_3^* \\ q_4^* \end{bmatrix}, \qquad (3)$$

where $[_iq]$ is a $(b \times 1)$ column matrix of generalised coordinates for blade i,

$[q_r^*]$ is a $(b \times 1)$ column of generalised coordinates of Coleman modes,

I is the $(b \times b)$ unit matrix,

0 is the $(b \times b)$ null matrix

and Ωt is the azimuth position of blade 1 from the aft direction, positive anti-clockwise looking down. The blades are numbered relative to blade 1 in the direction anti-clockwise looking down.

It will be seen that, with b modes assumed per blade, there are $4b$ Coleman modes for a four-bladed rotor. However, it is found that, with aerodynamic forces appropriate to the hover, q_1^* and q_3^* couple only with rigid body vertical translation, and *vice versa*, so that we may separate two systems, with no coupling between them:

(a) a system with vertical translation, q_1^* and q_3^* and

(b) the four remaining modes (a), (b), (d), (e) of Section 2.2 with q_2^* and q_4^*.

The system (a) plays no part in the air resonance phenomenon and is not considered further here.

With our assumptions for blade modes in Section 2.3.2, b is equal to 2, i.e. (flap and lag bending modes) since the blade pitch mode is used as a computational device for obtaining autostabiliser terms. Therefore the system (b) above is described in eight simultaneous equations, four corresponding to body modes and four to Coleman blade modes.

Apart from the property of eliminating periodic terms from the rotating inertia terms and from the aerodynamic terms in the hover, the Coleman transformations can be used to describe rotor distortions which are physically significant to an observer on the ground. For example, if we start with blade flapping as a blade mode, constant values of q_2^* and q_4^* are seen as fore-and-aft disc tilt, and lateral disc tilt. Similarly, starting with blade rotation as a blade mode, constant q_2^* and q_4^* are lateral and longitudinal cyclic pitch (*see* Section 3).

2.6. Form of Equations of Motion

Taking the definitions above, we obtain[4] the expressions for the equations of motion with the following simplifications:

(a) terms of order higher than (q) or (αq) are neglected, q being the generalised coordinates, α representing collective pitch, coning angle or induced flow and

(b) some terms factored by the blade chord, c, are neglected where there are similar terms factored by the distance of the section from the hub, r.

The form of the equations of motion is:

$$A\ddot{q} + \Omega B\dot{q} + D\dot{q} + \Omega^2 Cq + \Omega Fq + Eq = 0 \tag{4}$$

where A, B, C, D, E, F are (8×8) matrices, dimensional but scaled to give numerical values of order unity.

The matrices A to F are of the general form:

$$[X] = [X_0] + \alpha_0[X_1] + \beta_0[X_2] + \lambda[X_3]$$

and the contributions towards these matrices $[X_r]$ can be conveniently divided into

(a) rotating mass,

(b) aerodynamics and

(c) other (e.g. body mass, blade stiffness, gravitational).

The computer program[5] is arranged so that the three contributions can be separately called for, and so that the coefficients collective pitch α_0, coning angle β_0 and induced flow λ can be readily altered.

The solutions of equation (4) were obtained using a digital computer program[6] written to solve the fixed wing flutter equations. This program evaluates the complex roots of the equation for specific values of Ω, the rotor speed, and expresses the imaginary part of each root as a frequency, and the real part as the decay of an equivalent one degree of freedom system.

3. The Introduction of the Autostabiliser

3.1. The Inclusion of Cyclic Pitch

The autostabiliser to be included is taken to be a conventional type which applies cyclic pitch, having sensed body pitch and roll displacements and velocities, in order to stabilise the conventional helicopter instabilities in pitch and roll. Cyclic-pitch parameters can be identified as the Coleman mode equivalents to a particular blade mode. The Coleman transformations are introduced in Section 2.5. It is stated therein that only q_2^* and

q_4^* are retained in this work. From equation (3),

$$\begin{bmatrix} {}_1q \\ {}_2q \\ {}_3q \\ {}_4q \end{bmatrix} = \begin{bmatrix} I\cos\Omega t & I\sin\Omega t \\ -I\sin\Omega t & I\cos\Omega t \\ -I\cos\Omega t & -I\sin\Omega t \\ I\sin\Omega t & -I\cos\Omega t \end{bmatrix} \begin{bmatrix} q_2^* \\ q_4^* \end{bmatrix}.$$

Now cyclic pitch can be similarly described, using ${}_i\alpha$ as the blade incidence for blade i, and α_1, α_2 as cyclic pitch parameters

$$\begin{bmatrix} {}_1\alpha \\ {}_2\alpha \\ {}_3\alpha \\ {}_4\alpha \end{bmatrix} = \begin{bmatrix} \cos\Omega t & \sin\Omega t \\ -\sin\Omega t & \cos\Omega t \\ -\cos\Omega t & -\sin\Omega t \\ \sin\Omega t & -\cos\Omega t \end{bmatrix} \begin{bmatrix} \alpha_1 \\ \alpha_2 \end{bmatrix}.$$

Therefore, if we introduce a blade 'mode' q_c with uniform blade incidence, that is, $F_c(r) = 1$, then, from equation (1), we have

$$\psi_2 = q_c.$$

But the blade incidence ${}_i\alpha$ as defined above is the same as ψ_2, defined in equation (1). Therefore it may be seen from above that the cyclic pitch parameters α_1 and α_2 are, in fact, the Coleman equivalents of the 'mode' q_c. Therefore, by adding an artificial mode, with $F_c(r) = 1$ as its only deflection, to the general calculation procedure, we can evaluate the effects of cyclic pitch. This raises the order of the matrices in equation (4) to 10, but we are not interested in the generalised forces corresponding to these artificial modes and so the two equations corresponding to them may be removed. Also we are only interested in constant values of the artificial modes and thus in matrices C, F and E in equation (4). Finally, we take the extra columns of C, F and E due to the artificial modes, and these are found to contribute additional terms to (4):

$$[Q] = [\Omega^2[X] + \Omega[Y]] \begin{bmatrix} \alpha_1 \\ \alpha_2 \end{bmatrix} \tag{5}$$

where $[X]$ and $[Y]$ are of order (8×2).

3.2. Inclusion of the Autostabiliser Law

The autostabiliser law used in this analysis gives cyclic pitch applied to the rotor in terms of fuselage pitching and rolling angles and velocities.

$$\begin{bmatrix} \alpha_1 \\ \alpha_2 \end{bmatrix} = \begin{bmatrix} \sin\nu & -\cos\nu \\ -\cos\nu & -\sin\nu \end{bmatrix} \begin{bmatrix} k_1 + \dfrac{k_2 s}{1 + t_1 s} & 0 \\ 0 & k_3 + \dfrac{k_4 s}{1 + t_2 s} \end{bmatrix} \begin{bmatrix} \theta \\ \phi \end{bmatrix} \tag{6}$$

where θ is fuselage pitching angle,
ϕ is fuselage rolling angle,
ν, k_1, k_2, k_3, k_4, t_1, t_2 are autostabiliser constants and
s is the Laplace operator.

θ and ϕ can be expressed in terms of the generalised coordinates q describing body motion (*see* Section 2.2)

$$\begin{bmatrix} \theta \\ \phi \end{bmatrix} = \begin{bmatrix} \phi_P \\ \phi_R \end{bmatrix} [q]. \tag{7}$$

Equations (6) and (7) must be combined with equation (5) to yield the extra terms in the equations of motion (equation (4)), but the terms involving the Laplace operator require special attention[7] for the form of equation (4) to be maintained.

Combining equations (6) and (7), and rearranging

$$\left.\begin{aligned}\begin{bmatrix}\alpha_1\\ \alpha_2\end{bmatrix} &= \begin{bmatrix}\sin v & -\cos v\\ -\cos v & -\sin v\end{bmatrix}\begin{bmatrix}k_1 & 0\\ 0 & k_3\end{bmatrix}\begin{bmatrix}\phi_P\\ \phi_R\end{bmatrix}[q]\\ &+ \begin{bmatrix}\sin v & -\cos v\\ -\cos v & -\sin v\end{bmatrix}\begin{bmatrix}\dfrac{k_2 s}{1+t_1 s} & 0\\ 0 & \dfrac{k_4 s}{1+t_2 s}\end{bmatrix}\begin{bmatrix}\phi_P\\ \phi_R\end{bmatrix}[q]\end{aligned}\right\}. \tag{8}$$

Only the second term requires special attention. It may be put

$$\frac{1}{t_1 t_2}\begin{bmatrix}\sin v & -\cos v\\ -\cos v & -\sin v\end{bmatrix}\begin{bmatrix}k_2 s(1+t_2 s) & 0\\ 0 & k_4 s(1+t_1 s)\end{bmatrix}\begin{bmatrix}\phi_P\\ \phi_R\end{bmatrix}[q]\frac{t_1 t_2}{(1+t_1 s)(1+t_2 s)}. \tag{9}$$

It has been shown[7] that if we now define new coordinates $\hat{q}$ by

$$\begin{bmatrix}\sin v & -\cos v\\ -\cos v & -\sin v\end{bmatrix}\begin{bmatrix}\dfrac{k_2 s(1+t_2 s)}{t_1 t_2} & 0\\ 0 & \dfrac{k_4 s(1+t_1 s)}{t_1 t_2}\end{bmatrix}\begin{bmatrix}\phi_P\\ \phi_R\end{bmatrix}[q] = [\hat{q}]\frac{(1+t_1 s)(1+t_2 s)}{t_1 t_2} \tag{10}$$

where $\hat{q}$ is a (2×1) matrix,
then (9) becomes simply $\hat{q}$.

Now it may be seen that combining (5), (8) and (10) we obtain for additional terms to (4)

$$[Q] = [\Omega^2[X] + \Omega[Y]]\begin{bmatrix}\sin v & -\cos v\\ -\cos v & -\sin v\end{bmatrix}\begin{bmatrix}k_1 & 0\\ 0 & k_3\end{bmatrix}\begin{bmatrix}\phi_P\\ \phi_R\end{bmatrix}[q] + [\hat{q}] \tag{11}$$

and we have extra equations from (10). Expanding (10)

$$\left.\begin{aligned}&\begin{bmatrix}\sin v & -\cos v\\ -\cos v & -\sin v\end{bmatrix}\begin{bmatrix}\dfrac{k_2 s}{t_1 t_2} & 0\\ 0 & \dfrac{k_4 s}{t_1 t_2}\end{bmatrix}\begin{bmatrix}\phi_P\\ \phi_R\end{bmatrix}[q] + \begin{bmatrix}\sin v & -\cos v\\ -\cos v & -\sin v\end{bmatrix}\begin{bmatrix}\dfrac{k_2 s^2}{t_1} & 0\\ 0 & \dfrac{k_4 s^2}{t_2}\end{bmatrix}\begin{bmatrix}\phi_P\\ \phi_R\end{bmatrix}[q]\\ &= \begin{bmatrix}\left(\dfrac{1}{t_1 t_2}\right) + \left(\dfrac{t_1+t_2}{t_1 t_2}\right)s + s^2 & 0\\ 0 & \left(\dfrac{1}{t_1 t_2}\right) + \dfrac{(t_1+t_2)}{t_1 t_2}s + s^2\end{bmatrix}[\hat{q}]\end{aligned}\right\} \tag{12}$$

and interpreting sq as $\dot{q}$, and $s^2 q$ as $\ddot{q}$, (12) becomes

$$\left.\begin{aligned}&\begin{bmatrix}1 & 0\\ 0 & 1\end{bmatrix}_{\ddot{q}} + \begin{bmatrix}\left(\dfrac{t_1+t_2}{t_1 t_2}\right) & 0\\ 0 & \left(\dfrac{t_1+t_2}{t_1 t_2}\right)\end{bmatrix}_{\dot{q}} + \begin{bmatrix}\left(\dfrac{1}{t_1 t_2}\right) & 0\\ 0 & \left(\dfrac{1}{t_1 t_2}\right)\end{bmatrix}[\hat{q}]\\ &= \begin{bmatrix}\sin v & -\cos v\\ -\cos v & -\sin v\end{bmatrix}\begin{bmatrix}\dfrac{k_2}{t_1 t_2} & 0\\ 0 & \dfrac{k_4}{t_1 t_2}\end{bmatrix}\begin{bmatrix}\phi_P\\ \phi_R\end{bmatrix}[\dot{q}]\\ &+ \begin{bmatrix}\sin v & -\cos v\\ -\cos v & -\sin v\end{bmatrix}\begin{bmatrix}\left(\dfrac{k_2}{t_1}\right) & 0\\ 0 & \left(\dfrac{k_4}{t_2}\right)\end{bmatrix}\begin{bmatrix}\phi_P\\ \phi_R\end{bmatrix}[\ddot{q}]\end{aligned}\right\} \tag{13}$$

Equation (13) is now in the general form of equation (4), and solutions may be obtained in a similar way—*see* Section 2.6.

4. Solutions Obtained—No Autostabiliser

4.1. General Procedure

It is explained in Section 2.6 that the computation for the equations of motion was arranged so that the contributions from various sources and with various values of the parameters, coning angle β_0, collective pitch α_0 and induced flow λ, could be readily obtained. This procedure was used to obtain solutions with various combinations of parameters in order to explore the sensitivity of the results to these parameters. This procedure often resulted in the obtaining of solutions for unrealistic combinations of parameters, for instance, finite coning angle with zero collective pitch. This was regarded as unimportant compared with the advantages of the procedure in enabling the sensitivities of the system to reasonably well defined physical parameters to be found.

4.2. Solution with no Aerodynamic Forces and Zero Collective Pitch

This solution could be regarded as the solution in a vacuum and in a zero gravity field. Fig. 5 shows, for a range of rotor speeds, the roots of equation (4), expressed as frequencies (relative to an axis set fixed to earth) and decays (*see* Section 2.6). Apart from the roots shown, there are six zero roots. The roots marked A and B can be identified from their associated vectors as predominantly lag bending modes. The roots marked C, D and E are best identified by the solutions of subsidiary systems. Fig. 6 shows the solutions for the four body modes only, i.e. with the rotor behaving as a rigid disc. As with Fig. 5, apart from the root shown, there are six zero roots. Fig. 7 shows the solutions for the blade-flap bending modes only, and Fig. 8 shows the solutions for the body modes with blade-flap bending. Comparing Figs. 5 and 8, there can be little doubt that roots D and E are combinations of a body mode, with the body inertia being reacted by the gyroscopic property of the rotor, and of blade-flap bending.

Figure 5 indicates that instabilities occur for rotor speeds at which the frequency of the lower frequency lag bending mode coalesces with those of modes involving body motions. This is a well-known property of systems in ground resonance and air resonance—*see* Refs. 1, 2 and 3. The frequencies of the instabilities are well below the lowest structural frequency of the fuselage. There is, therefore, no urgent reason to change the assumption of a rigid fuselage made in Section 2.2. It may be seen from Fig. 5 that there is instability for a range of rotor speeds around the standard scaled operating value of 3·33, and that this rotor speed range could be shifted by changing the zero rotor speed lag-bending-mode frequency. These results are similar to those found[2,3] for similar systems with a 'soft' lag bending mode, i.e. one with a lag-bending-mode frequency lower than the standard operating rotor speed.

4.3. Solutions Including Aerodynamic Forces

Figure 9 shows the solution for the system with aerodynamic forces and with values of α_0, β_0 and λ that are consistent with the assumptions of Section 2.3.1 and are appropriate to a rotor thrust equal to the weight of the aircraft at the standard scaled rotor operating speed, 3·33. Strictly these values should only be used for the solution at a scaled rotor speed of 3·33. [A constant value of α_0 leads to a rotor thrust varying with Ω^2. With this thrust variation, a constant value of β_0 is appropriate, but the induced flow λ should then vary with Ω. Therefore, our solution values of α_0, β_0 and λ cannot be strictly matched to a physically realistic combination except at the scaled rotor speed 3·33.]

Apart from the roots shown on Fig. 9, there are two zero roots and two very low frequency oscillations.

Comparing Figs. 5 and 9, it can be seen that the aerodynamic forces result in very large damping in the modes D and E, and large damping in mode C. In Section 4.2 it was shown that these modes involved body modes and blade-flap bending. The frequencies of modes C and E are not greatly changed, but mode D is so heavily damped that at scaled rotor speeds above 1·9, the oscillation becomes a pair of subsidences. The lag modes A and B attract little aerodynamic damping, so that the instability of Fig. 5 with no aerodynamic damping still exists on Fig. 9, and the rotor speed range for the instability is wider.

For further solutions, the presentation of Figs. 5 and 9 is changed so that all that is shown is the decay of the lower frequency lag mode A. The frequencies of all the modes and the decays of the modes other than mode A are changed by small amounts in these further solutions. The presentation of decay of lag mode A is also changed. The fraction of critical damping shown in Figs. 5 and 9 is directly related to the cycles to half or double amplitude. At rotor speeds close to 1·6 the lag mode frequency (referred to earth axes) is close to zero, and is changing rapidly with rotor speed. Therefore, if the decay of the mode is described by the cycles to half amplitude, the large proportional frequency variations with rotor speed will manifest themselves in the large changes in the decays shown in Fig. 9 for rotor speeds just below 2·0. This effect is avoided if the decays are presented as the *time* to half or double amplitude, and Fig. 10 gives the reciprocal of these times.

On Fig. 10 the solutions with various aerodynamic or mass effects included are shown. These solutions were obtained by including, in the equations of motion, various combinations of collective pitch α_0, coning angle β_0 and induced flow λ, the numerical values of these being the standard values appropriate to a scaled rotor speed of 3·33.

Curve (a) is the result with no aerodynamic forces, zero collective pitch α_0, zero coning angle β_0—it is the equivalent of Fig. 5.

Curve (b) has aerodynamic forces, zero collective pitch, zero coning angle and zero induced flow.

Curve (c) is as curve (b) with the mass and aerodynamic contributions associated with coning angle β_0.

Curve (d) is as curve (c) with the aerodynamic contributions only of collective pitch α_0 and induced flow λ.

Curve (e) is as curve (d) with the additional mass contributions of collective pitch α_0. This curve is the equivalent of Fig. 9.

Also shown on Fig. 10 is a line labelled '0·5 per cent blade damping'. The value refers to the structural damping of a blade when non-rotating, and it has been checked that a rough indication of the effect of blade structural damping in the lag mode can be obtained by taking this line as the datum rather than the horizontal axis. For other values of blade structural damping, other lines may be drawn at proportional distances from the horizontal axis.

It may be seen that, relative to the amount of structural damping that may be expected in a non-articulated blade (0·5 to 1 per cent of critical damping), there is a large variation in the degree of stability or instability due to the effects introduced in Fig. 10. The biggest effects found are those due to the aerodynamic contributions only of α_0 and λ (Curve (c) to Curve (d)), and those due to the mass contribution only of α_0 (Curve (d) to Curve (e)). A study of the coefficients of the equations of motion arising from these effects resulted in a comparatively simple physical picture of the working of these effects, and these are described below.

4.4. The Consequences of Collective Pitch and Induced Flow in the Aerodynamic Terms

The introduction of α_0 and λ in aerodynamic terms results in a change from Curve (c) to Curve (d) in Fig. 10.

Section 2.4 and Fig. 4 describe the assumptions made in the derivation of the aerodynamic terms. A detailed study of the coefficients of the equations of motion shows that the major aerodynamic terms dependent upon α_0 and λ can be explained by the restricted case shown in Fig. 11. In Fig. 11, the total lift on the blade section is made up of

(a) the steady lift $\rho c l_\alpha[r^2\Omega^2\alpha_0 - r\Omega\lambda]$ and

(b) the perturbation lift $-\rho c l_\alpha r\Omega\,\dot{z}$

The most important term is the generalised aerodynamic force in the lag bending mode and, ignoring the small term due to the aerodynamic drag of the section, this is derived from the work done in a small displacement δx, that is from

$$L\varepsilon\delta x$$

or, from

$$\rho c l_\alpha[r^2\Omega^2\alpha_0 - r\Omega\lambda - r\Omega\dot{z}]\left[\alpha_0 - \frac{\lambda}{r\Omega} - \frac{\dot{z}}{r\Omega}\right]\delta x. \tag{14}$$

The linearised equations of motion (*see* Section 2.6) retain only the terms

$$(\alpha_0\dot{z}\delta x) \qquad \text{and} \qquad (\lambda\dot{z}\delta x),$$

and equation (14) shows that there are two contributions to these terms;

(a) one due to the steady lift $\rho c l_\alpha(r^2\Omega^2\alpha_0 - r\Omega\lambda)$ being inclined by the effect of the perturbation velocity $\dot{z}$ on the inclination of the airflow relative to the lag bending direction δx, and

(b) the other due to the perturbation lift $\rho c l_\alpha r\Omega\dot{z}$ being inclined by α_0 and λ relative to the lag bending direction δx.

In order to check that this simplified analysis revealed the basis of the sensitivity, full solutions, corresponding to Curve (e) of Fig. 10, were obtained with the modified assumption that the steady-lift direction was *not* changed by the perturbation velocity $\dot{z}$ but remained normal to the *steady* airflow. It is emphasised that the magnitude of the lift remained constant, but its assumed direction was changed. Obviously a change in the magnitude of the lift would have important effects as well. This solution is shown in Fig. 10 as Curve (f). It should be compared with Curve (e), for which the same assumptions apply except the assumed direction of the steady lift. The differences between Curves (e) and (f) are significant relative to blade structural damping. Thus the general accuracy of representation of the effects shown on Fig. 11 is important, and attention is drawn to the accuracy likely to have been obtained in this work, bearing in mind

(a) assumptions made for computational simplicity (constant spanwise α_0 and uniform induced flow λ) and

(b) basic difficulties in ensuring accurate representation of the component of the lift in the lag bending direction.

4.5. The Consequences of Collective Pitch in the Mass Terms

The introduction of α_0 in mass terms results in a change from Curve (d) to Curve (e) in Fig. 10. The physical effects of α_0 in the mass terms can be seen from the shapes of the blade normal modes.

The equations in this work are of a form for which blade normal modes exist, if the blade coning angle β_0 is taken as zero. The deflections at the blade tip in the normal modes at a scaled rotor speed of 3·0 are shown in Fig. 12. Fig. 12 shows the blade deflections in the vertical and horizontal directions, and the steady position of the blade-section datum-line is also shown. It may be seen that the collective pitch angle α_0 results in small differences of about 0·03 radians in the inclination of the blade tip in the normal modes. These differences are the main cause of the differences between Curves (d) and (e) in Fig. 10. Such a sensitivity casts immediate doubts about the accuracy that can be achieved with the assumptions for mode shapes made in Section 3.2. There it is explained that the flap and lag modes assumed are the flap and lag parts only of the predominantly flap and lag normal modes. Obviously, in view of the sensitivity of the results to lag-mode shape, the datum-normal modes should be represented more carefully. This could be done simply in this work by introducing the datum-normal modes, at a rotor speed in the instability range, as coupled flap and lag modes. However, this process would achieve only the accuracy of the mode shapes at the standard rotor speed chosen for the computation of the blade-normal modes, and not for the range of rotor speeds for which results are presented. For this reason, results with a more accurate handling of the blade-normal modes are not presented. It is considered that the main conclusion from this part of the analysis is that the stability in air resonance is very sensitive to the small amount of flap bending in the predominantly lag-bending mode.

5. Solutions Obtained–With Autostabiliser

The autostabiliser with the law described in Section 3 is introduced into the case with no autostabiliser that is shown on Fig. 9 and as Curve (e) on Fig. 10. The frequencies and decays with autostabiliser are shown on Fig. 13, and, when these are compared with Fig. 9 it is seen that

(a) the frequency of body mode E has been appreciably increased by the autostabiliser,

(b) the decay of body mode E has been considerably reduced by the autostabiliser and

(c) the decay of body mode D has been reduced by the autostabiliser, the mode remaining a heavily damped oscillation in Fig. 13, rather than the subsidence in Fig. 9.

Fig. 14 shows that the stability of air resonance has been made significantly worse by the autostabiliser.

The autostabiliser was not added to the other cases of Fig. 10 because there is no reason to believe that the sensitivities discussed in Section 4 with no autostabiliser will not be present with the stabiliser. It is fair to conclude, therefore, that the autostabiliser with a law of the form of equation (6) will be destabilising, but that the absolute stability of the aircraft with autostabiliser will depend upon the action of the blade structural and aerodynamic parameters discussed in Section 4.

6. Discussion of Accuracy Being Achieved

Section 4.5 and Fig. 12 show how the stability in air resonance depends critically on the small amount of flap bending in the predominantly lag-bending (fundamental) mode of the blades. The blade may be regarded as a twisted beam, the twist being either built-in or due to the steady forces acting on it, and the coupled flap-lag motion of such a beam is not easily represented. Sophisticated calculation procedures exist for the determination of the modes of the blade, but it is thought that, while there is general satisfaction at the accuracy with which these predict modal frequencies, the much more difficult determination of accurate mode shapes has been put to few checks against experiment due to the difficulties in measuring mode shapes of rotating blades. Therefore, in view of the significant variation in stability brought about by small changes in the lag-bending-mode shape, it is difficult to find adequate confidence in the accuracy of blade mode representation to accept without reservation any calculation showing freedom from air resonance instability.

Section 4.4 and Fig. 11 show that there is also critical dependence on the accuracy of aerodynamic data. The inclination of the steady lift due to blade perturbation velocities, and the inclination of perturbation lift due to induced flow, as well as the magnitude of the lift, all depend, for accurate estimation, on accurate distributions of steady lift, induced flow and perturbation lift over the rotor disc. It certainly cannot be taken for granted that adequate accuracy is achieved with the assumptions made here of strip theory and uniform induced flow.

With doubts about the accuracy of blade-structural and rotor-aerodynamic data, it must be concluded that a calculation for air resonance cannot be relied on with the confidence necessary with a potentially dangerous instability, until some experimental evidence supports the accuracy of the data or until the overall results of the calculation have been correlated satisfactorily with an experimental check on the stability of the aircraft, or of a dynamically similar model.

A practical alternative would be the fitting of lag dampers to the blades so that the total blade damping would be greater than the worst instability predicted by calculations—*see* Section 4.3 and Fig. 10.

Artificial lag damping may not always prove necessary,[2,3] and it has been shown[2] that it is possible to calculate with good accuracy and obtain good, positive correlation with flight tests.

7. Checking of Data or Technique by Model Experiments

Section 6 refers to the need for experimental checks before the accuracy of a calculation can be relied upon. It is useful, therefore, to discuss the possibility of making experiments on dynamically similar models to provide the required checking of calculation data or technique.

The simplest model test would be one on a single dynamically similar blade with a fixed shaft, if a suitable test parameter could be identified. The total structural and aerodynamic damping in the blade-lag mode would be comparatively simple to measure. The correlation between air-resonance stability and the aerodynamic damping in the blade lag mode was found from this study and is shown in Fig. 15. On Fig. 15, 'air-resonance stability' is represented by the real part of the root corresponding to A of Fig. 9 at a scaled rotor speed of 3·0. This quantity is inversely proportional to time to half amplitude, for instance. It may be seen that the correlation is not unreasonable, but that this correlation is not of the intuitive type, in that the higher the lag-mode aerodynamic damping, the worse the air-resonance stability. With blade-structural damping, it has been established that, approximately, the level of air-resonance stability is increased by the amount of blade-structural damping introduced. Obviously the role of aerodynamic damping is much more complicated than this, and, for this reason, the aerodynamic damping in the lag mode is not considered to be a suitable criterion for air-resonance stability.

The most complicated model would be a dynamically similar rotor system mounted on a fuselage with body freedoms. A fuselage reasonably representative in mass but made unrepresentatively stiff would suffice. Such a model could be tested for air resonance stability, but for adequate correlation with calculations using the model data, it would be necessary to measure the lag-mode damping, or to arrange parameters so that critical stability boundaries were observed. A simple comparison of a stable model with stability in the calculations would not be adequate.

Another possibility is the measurements of model rotor 'impedances'. A rig has been described[8] in which a model rotor system can be forced in prescribed body freedoms, one at a time, and the forces corresponding to all the body freedoms measured. These force measurements which vary with rotor speed and with the impressed, or excitation, frequency, can be assembled in matrices of 'stiffness coefficients' or 'impedances'. The model rotor to be tested in such a rig would be as comprehensive as that required for an air-resonance model, but it is possible that the comparison between calculated and measured impedance values could be more conducive to empirical modifications to the calculations for better agreement than the comparison of calculated and measured air-resonance stability boundaries or lag-mode dampings. In order to assess this possibility the impedances associated with the various rotor representations in this study were found. Of the impedances, it was found that some, in particular, showed larger differences between the different cases. One of these is shown as a complex quantity in Fig. 16. The curves are identified by the same letters that identify the cases in the stability results of Fig. 10. The excitation frequency for these cases varied from just below to just above the rotor lag-mode frequency at a scaled rotor speed of 3·0. It may be seen that there are considerable differences between the impedances for the different cases, and it may be concluded that these impedances are sensitive enough to be a basis for checking a theoretical representation against measurements. Whether any differences between theoretical values and measurements can be interpreted so that improvements can be made to the theory must await a set of measurements.

8. Conclusions

The equations of motion for a helicopter in the hover were set up, for an assumed set of rigid body modes and of blade-flap and lag-bending modes. The use of the Coleman transformations[1] resulted in a set of equations with no periodic coefficients. Simple blade aerodynamic assumptions were made; in particular, strip theory was used and induced flow was taken as uniform over the disc.

Solutions indicated that the stability of the motion described[2,3] as air resonance was very sensitive to parameters describing collective pitch and induced flow. Similar parameter variations were made in intermediate solutions, in order to try to establish some connection between stability and physical properties of the system.

It has been concluded that, although blade structural damping alleviates instability, the expected level of structural damping is not significant in regard to the degree of instability that may occur, and that blade structural damping cannot be relied upon to stabilise the system.

It has been shown that the stability of the system is very sensitive to

(a) the small amount of flap bending in the predominantly lag bending normal mode of the blades, and

(b) the inclination of the blade lift to the lag bending direction, and the distribution of the lift.

Item (b) requires accurate data for the blade incidence distribution (built-in twist, steady twist and induced flow) and for the basic aerodynamic theory.

It has been concluded that, in view of (a) and (b) above, a calculation for air resonance cannot be relied on until some experimental evidence supports the accuracy of the data, or until the calculation technique has been checked by a positive correlation with full scale flight model tests. In the absence of either of these, an alternative would be the fitting to the blades of artificial lag damping, which could possibly be reduced or removed after quantitative measurements of the damping in flight of the predominantly lag-bending mode. Artificial damping is not necessarily required for stability,[2,3] but the seriousness of the potential instability and the relative ineffectiveness of natural blade damping require a cautious interpretation of theoretical work until experimental results have provided a good, positive correlation with the theoretical work.

An assessment has been made of experimental data checks that could be made before an aircraft is available for flight testing. The testing of a dynamically similar model has obvious value. It has also been shown that impedance measurements on a dynamically similar rotor system show promise of providing a useful basis for checking the accuracy of a theoretical representation.

LIST OF SYMBOLS

A, B, C, D, E, F	Matrices of coefficients in equations of motion (4)
b	Number of blade modes assumed
c	Blade chord
C_D	Drag coefficient
D	Drag per unit length of blade
fq, gq, Fq	Deflections—*see* equation (1) and Fig. 2
I	Unit matrix
k_1, k_2, k_3, k_4	Autostabiliser constants
l_α	Lift curve slope—*see* Fig. 4
L	Lift per unit length of blade
${}_iq$	Generalised coordinate for blade i
q_r^*	Generalised coordinates associated with Coleman modes—*see* equation (3)
$\hat{q}$	Generalised coordinates used in autostabiliser representation—*see* equation (10)
r	Radius of blade section from hub
s	Laplace operator
t_1, t_2	Autostabiliser constants
v_1, v_3	Components of velocity of blade section
δx	Blade section deflection in lag direction—*see* Fig. 11
X, Y	Matrices used in autostabiliser representation—*see* equation (5)
$\dot{z}$	Blade section velocity in flap direction—*see* Fig. 11
$\bar{O}X_{Br}$	Orthogonal set of axes in Fig. 1
PX_{Cr}	Orthogonal set of axes in Fig. 2
$\bar{P}X_{Dr}$	Orthogonal set of axes in Fig. 2
α_0	Collective pitch, defined in Fig. 1
α_1, α_2	Cyclic pitch
β_0	Coning angle, defined in Fig. 1
ε	Angle defined in Fig. 11
θ	Fuselage pitching angle
λ	Induced velocity
ν	Autostabiliser constant
ρ	Density of atmosphere
ϕ	Fuselage rolling angle
ψ_r	Euler angles defined in equation (1)
Ω	Scaled rotor rotational speed
$\cdot$	Denotes $\frac{d}{dt}$
$\cdot\cdot$	Denotes $\frac{d^2}{dt^2}$

REFERENCES

No.	*Author(s)*	*Title, etc.*
1	Robert P. Coleman and Arnold M. Feingold	Theory of self-excited mechanical oscillations of helicopter rotors with hinged blades. N.A.C.A. Report 1351 (1958).
2	R. E. Donham, S. V. Cardinale and I. B. Sachs	Ground and air resonance characteristics of a soft in-plane rigid rotor system. *J. Amer. Helic. Soc.*, 14(4) (1969).
3	R. T. Lytwyn, W. Miao and W. Woitsch	Airborne and ground resonance of hingeless rotors. *J. Amer. Helic. Soc.*, 16(2) (1971).
4	J. C. A. Baldock	The linearised equations of motion of a flexible helicopter body plus rotor system using a semi-rigid representation: Part 1—General Theory. Unpublished M.O.D.(P.E.) material.
5	R. J. Davies	The linearised equations of motion of a flexible helicopter body plus rotor system using a semi-rigid representation: Part 2—Digital computer program. To be published.
6	Ll. T. Niblett	Methods of solving the flutter equations in use at R.A.E. A.R.C. C.P.1046 (1968).
7	A. D. N. Smith	The analytical solution of flutter equations involving power operated controls. Unpublished M.O.D.(D.E.) material.
8	R. Cansdale, D. R. Gaukroger and C. W. Skingle	A technique for measuring impedances of a spinning model rotor. R.A.E. Technical Report 71092 A.R.C. 33498 (1971).

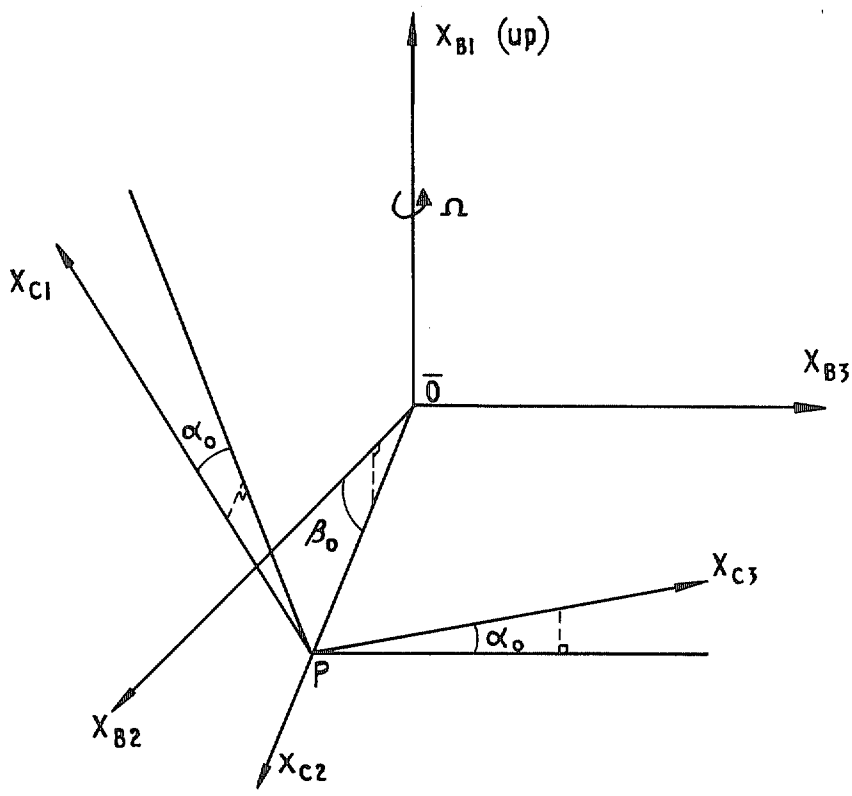

FIG. 1. Axis system showing definition of 'coning angle' β_0 and 'collective pitch' α_0.

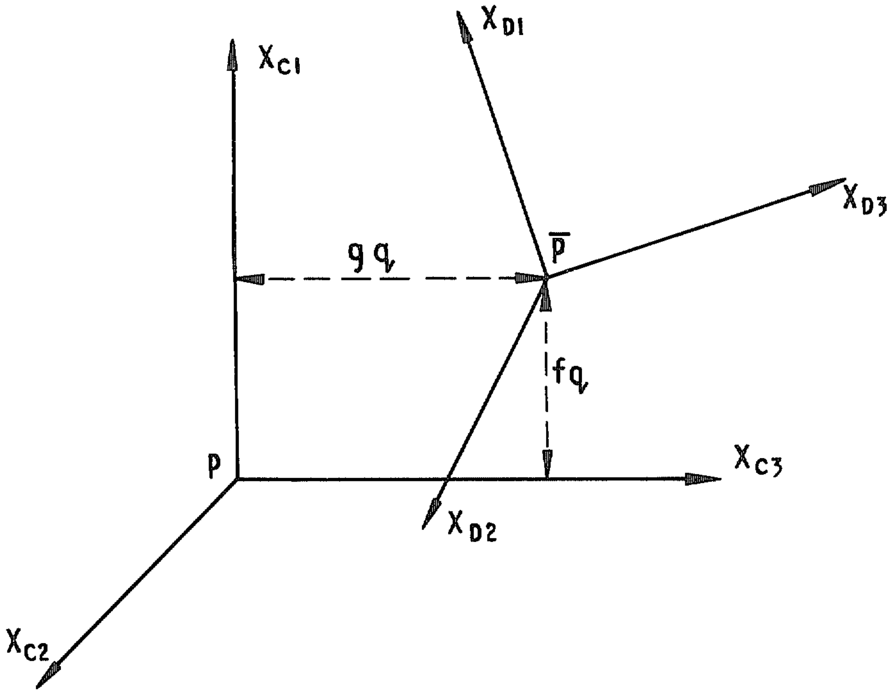

FIG. 2. Axis system showing definition of deformation coordinates q.

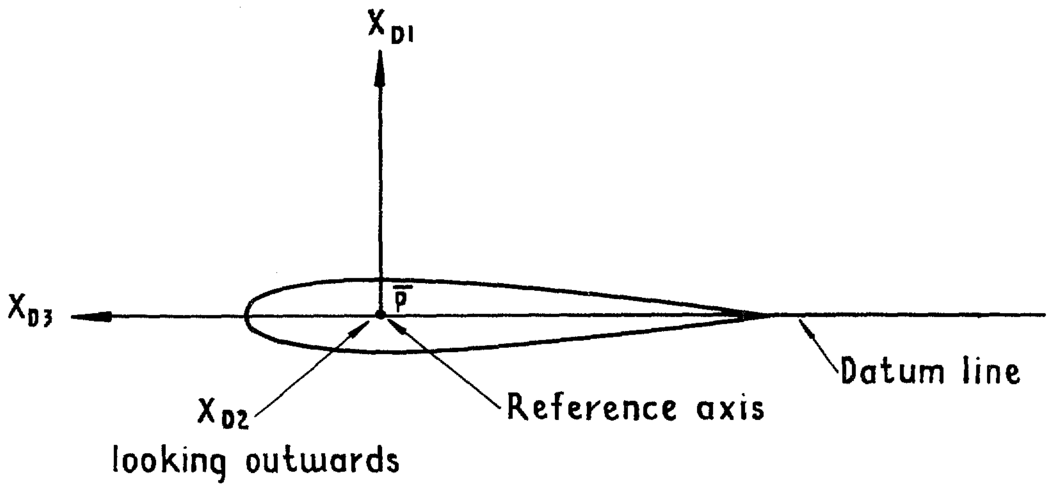

FIG. 3. Axes $\bar{P}X_{Dr}$ on a typical section.

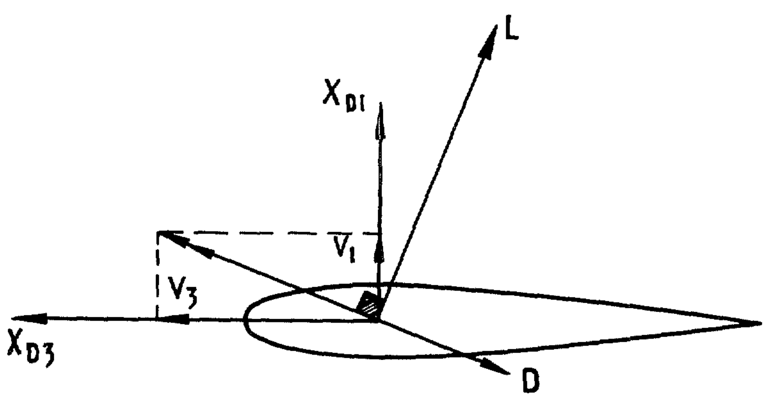

$L = -\rho V_1\ V_3\ c\ell_\alpha$ per unit span

$D = \frac{1}{2}\rho c\left(V_1^2 + V_3^2\right)\ C_D$ per unit span

FIG. 4. Definition of aerodynamic forces.

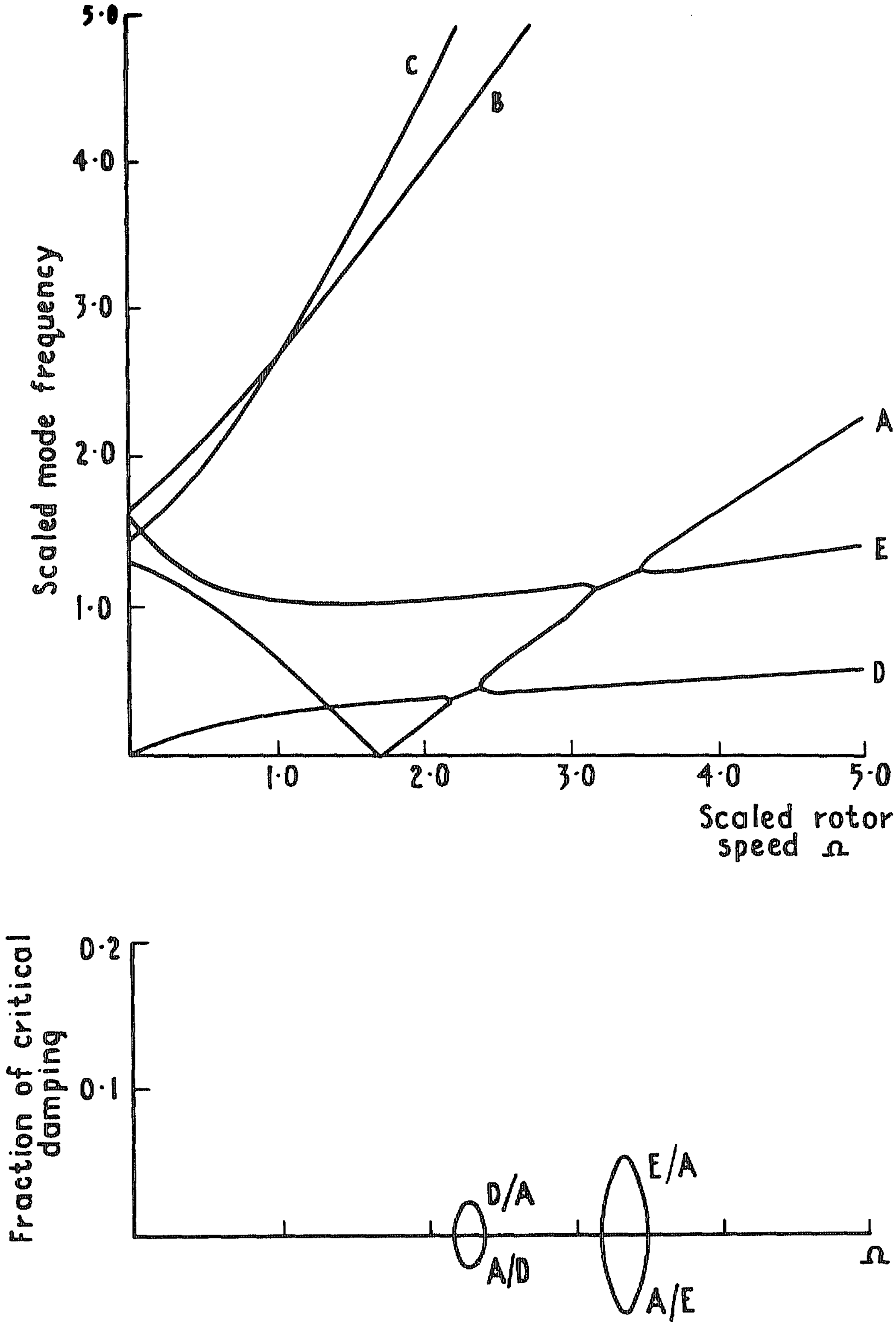

FIG. 5. Variation of mode frequency and damping with rotor speed—case with no aerodynamic forces.

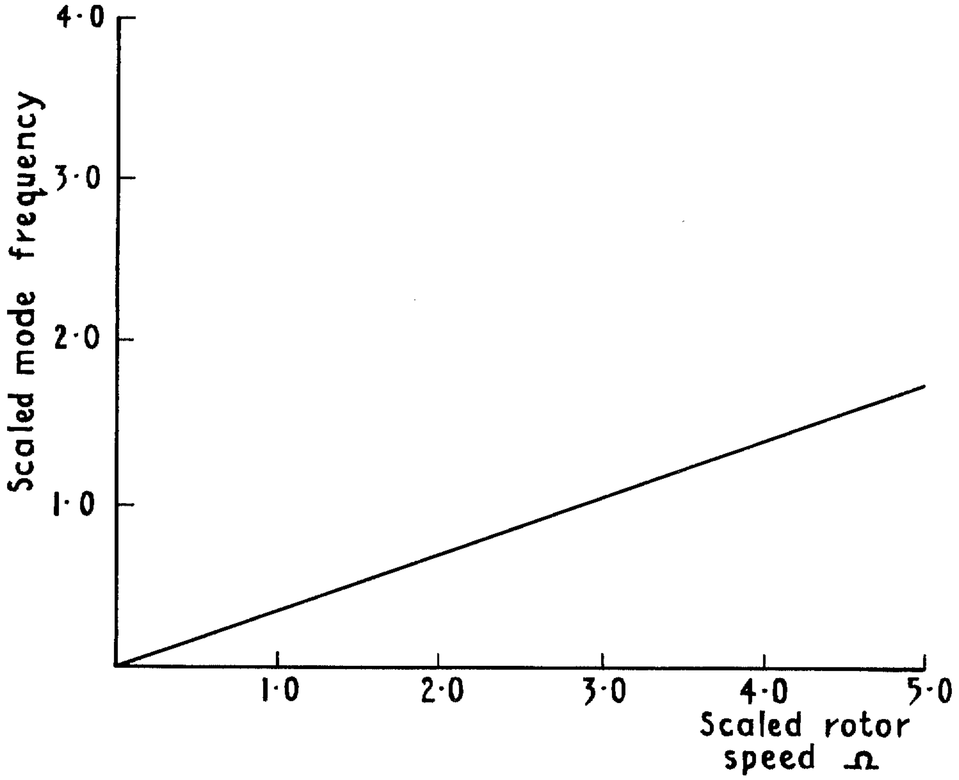

FIG. 6. Variation of mode frequency with rotor speed—case with body modes only and no aerodynamic forces.

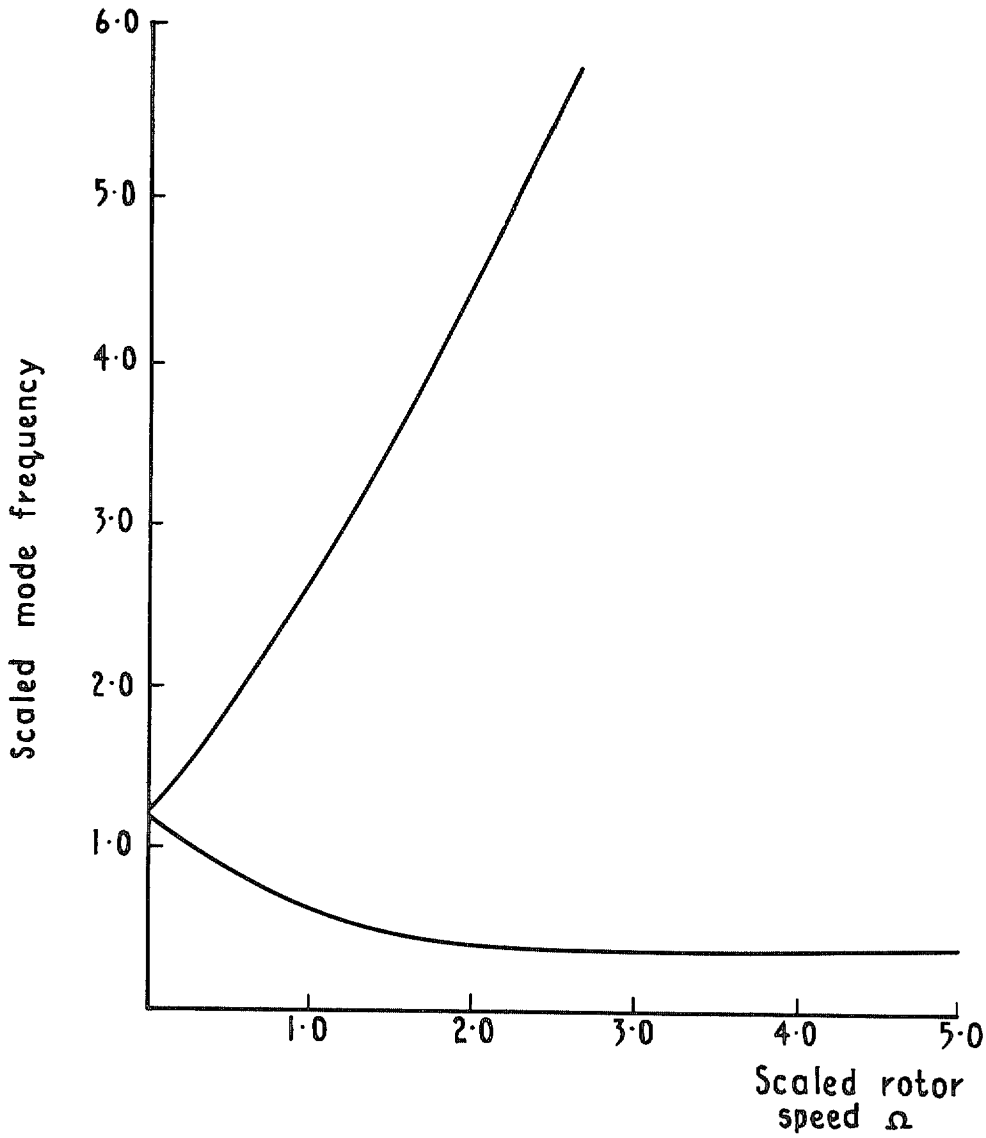

FIG. 7. Variation of mode frequency with rotor speed—case with blade flap bending modes only and no aerodynamic forces.

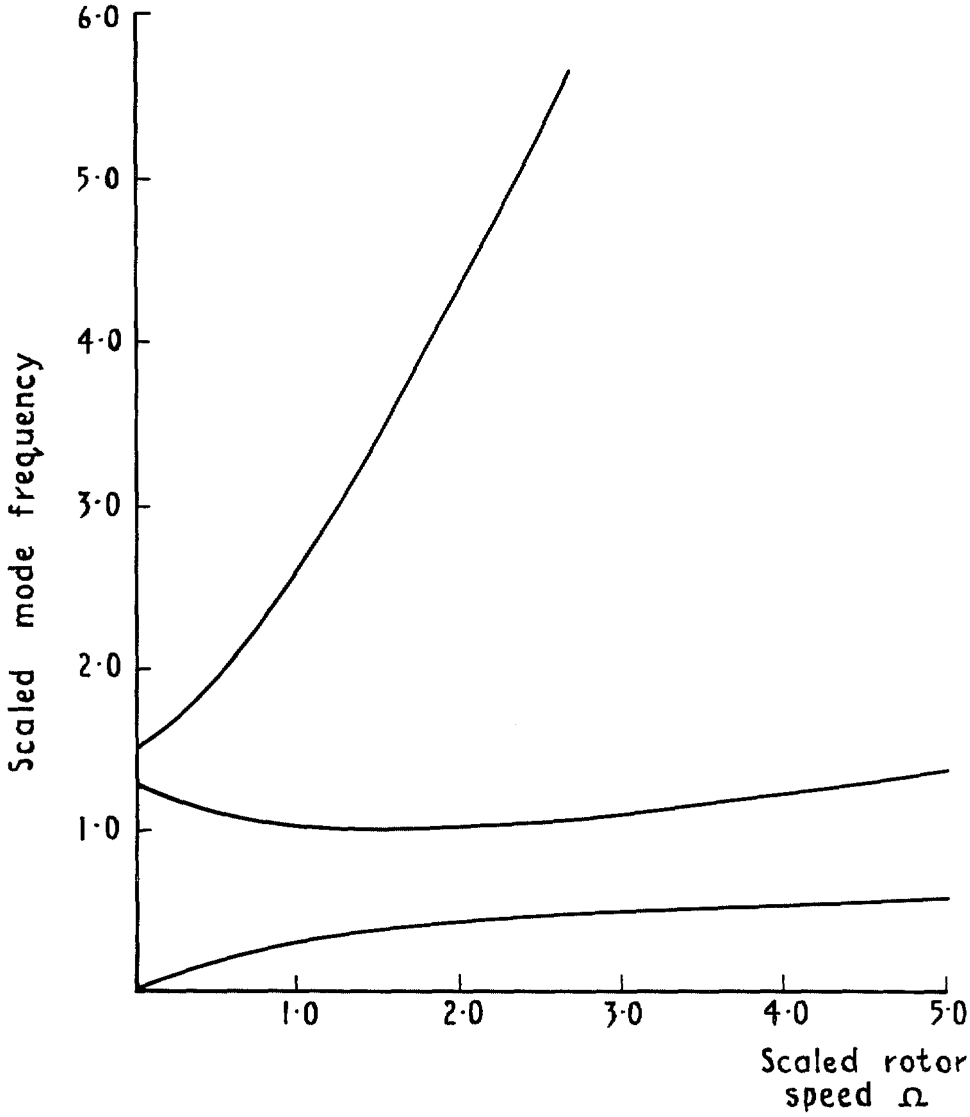

FIG. 8. Variation of mode frequency with rotor speed—case with body modes and blade flap bending modes only and no aerodynamic forces.

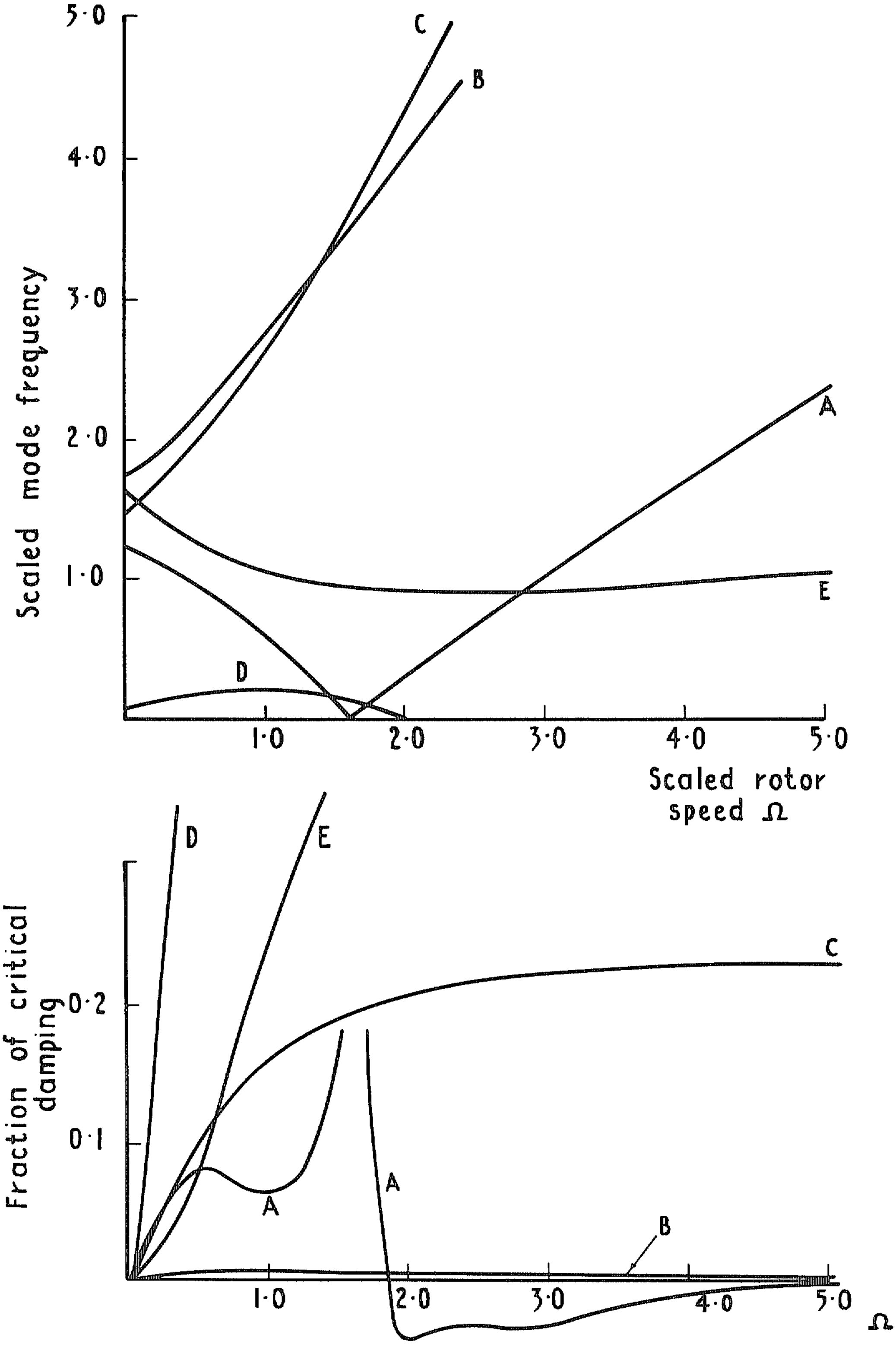

FIG. 9. Variation of mode frequency and damping with rotor speed—case with aerodynamic forces and finite coning angle, collective pitch and induced flow.

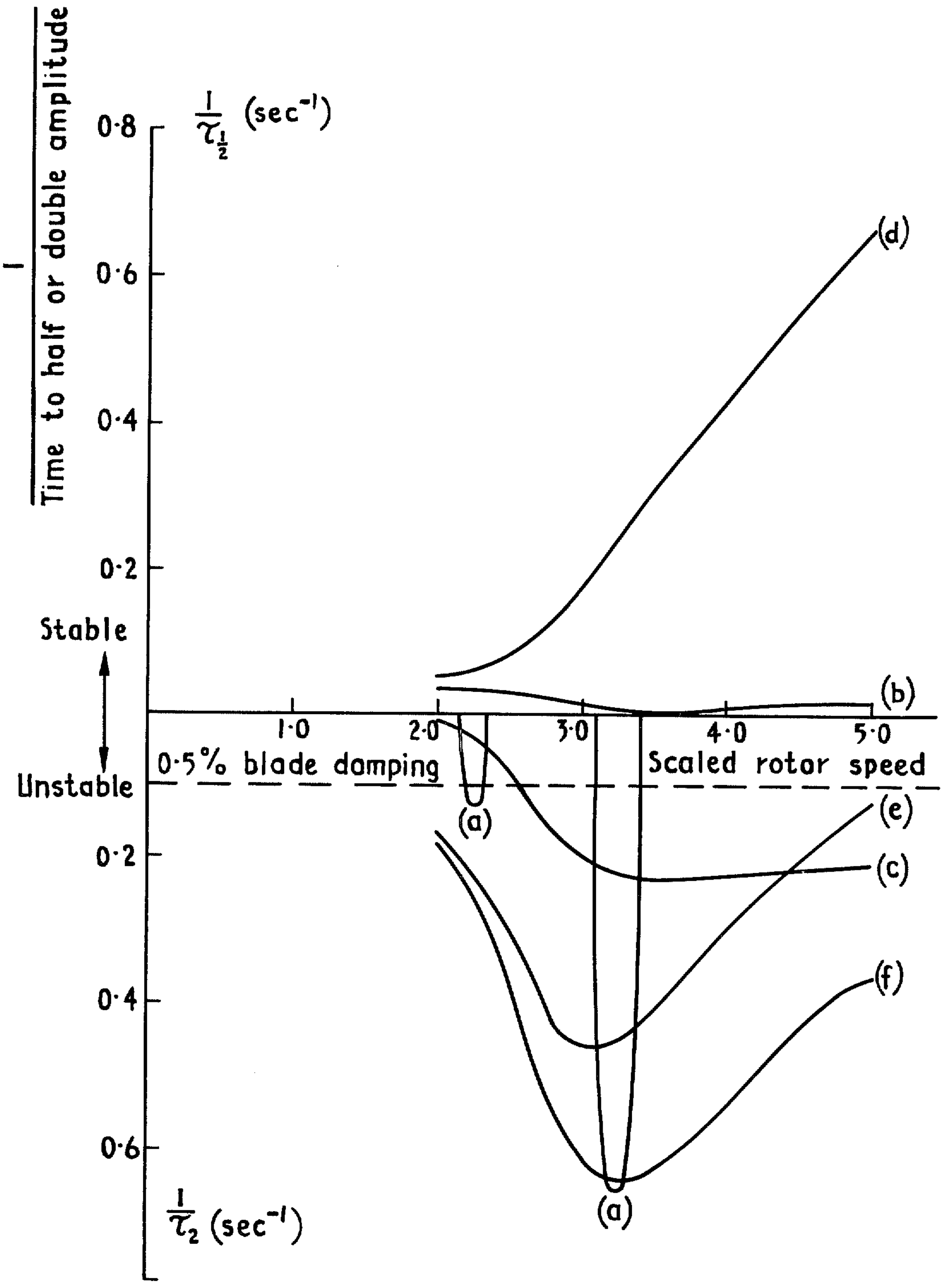

FIG. 10. Variation of decay of lag mode (A) with rotor speed for cases defined in Section 4.3.

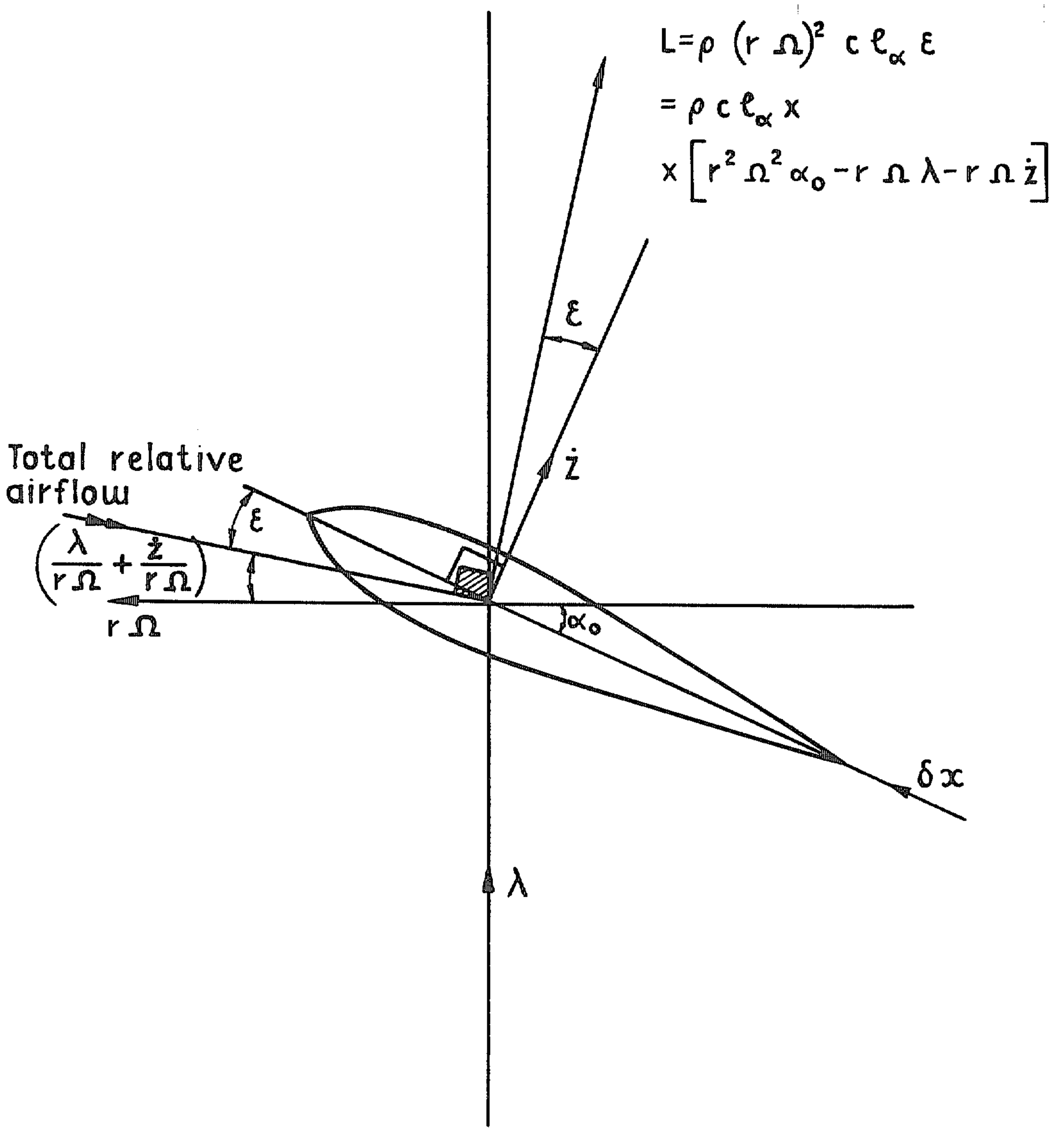

FIG. 11. Aerodynamic forces for a restricted case discussed in Section 4.4.

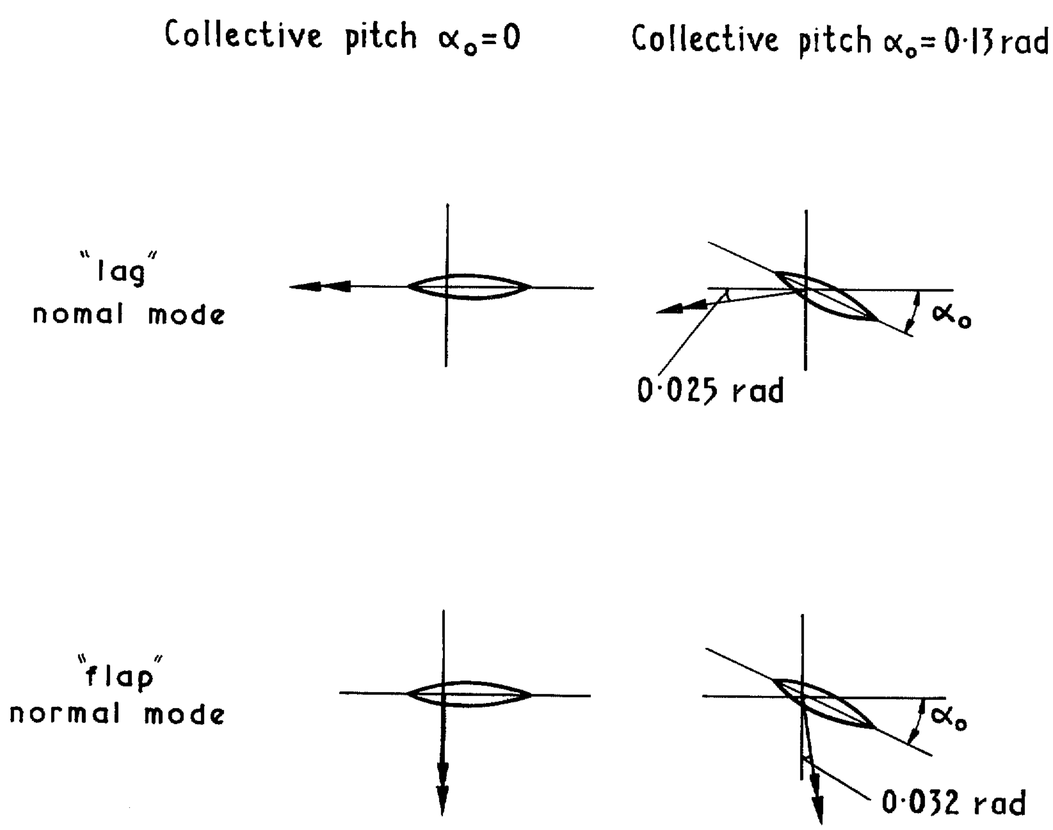

FIG. 12. Blade tip deflections in normal modes—scaled rotor speed = 3·0.

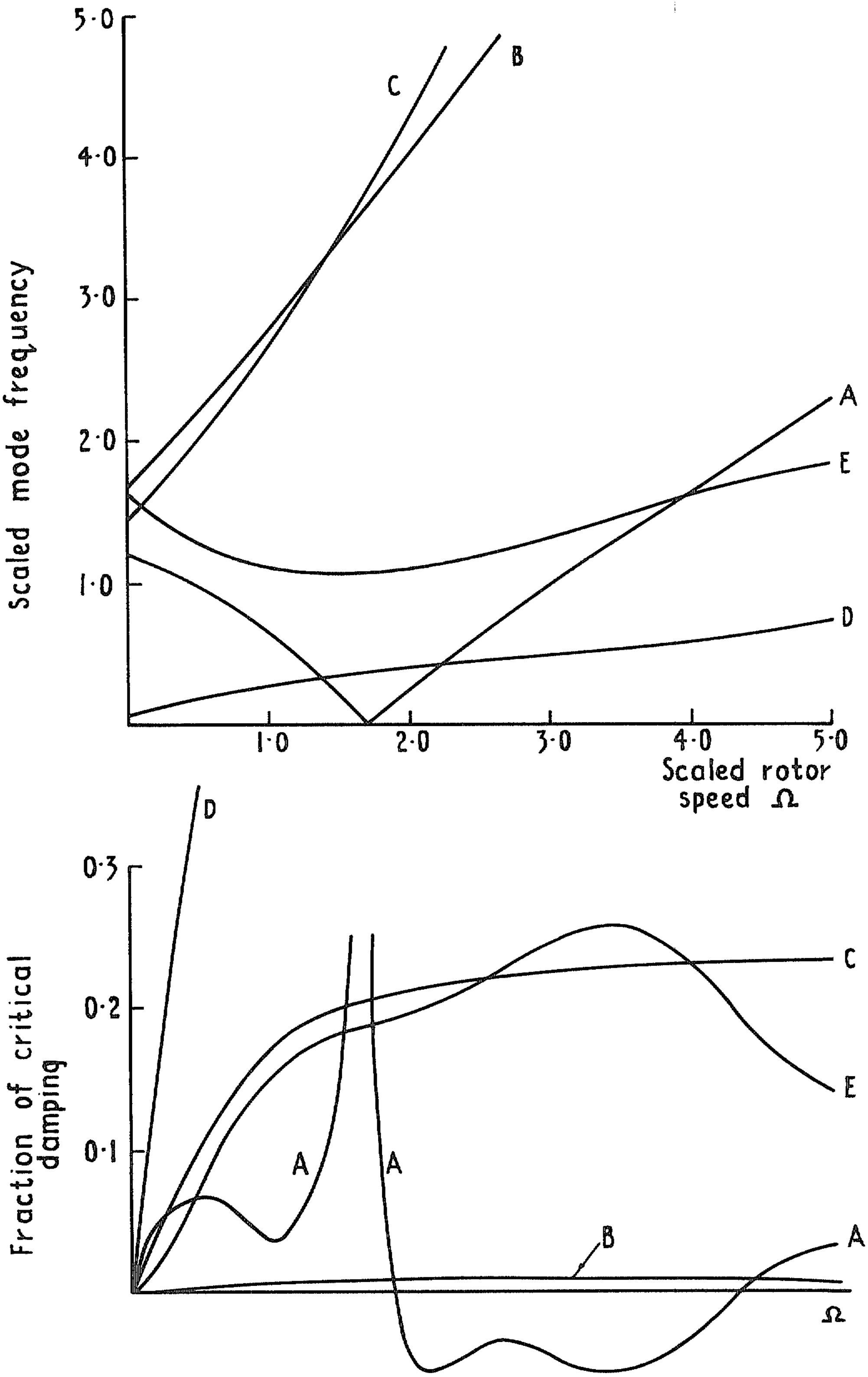

FIG. 13. Variation of mode frequency and damping with rotor speed—case of Fig. 9 plus autostabiliser.

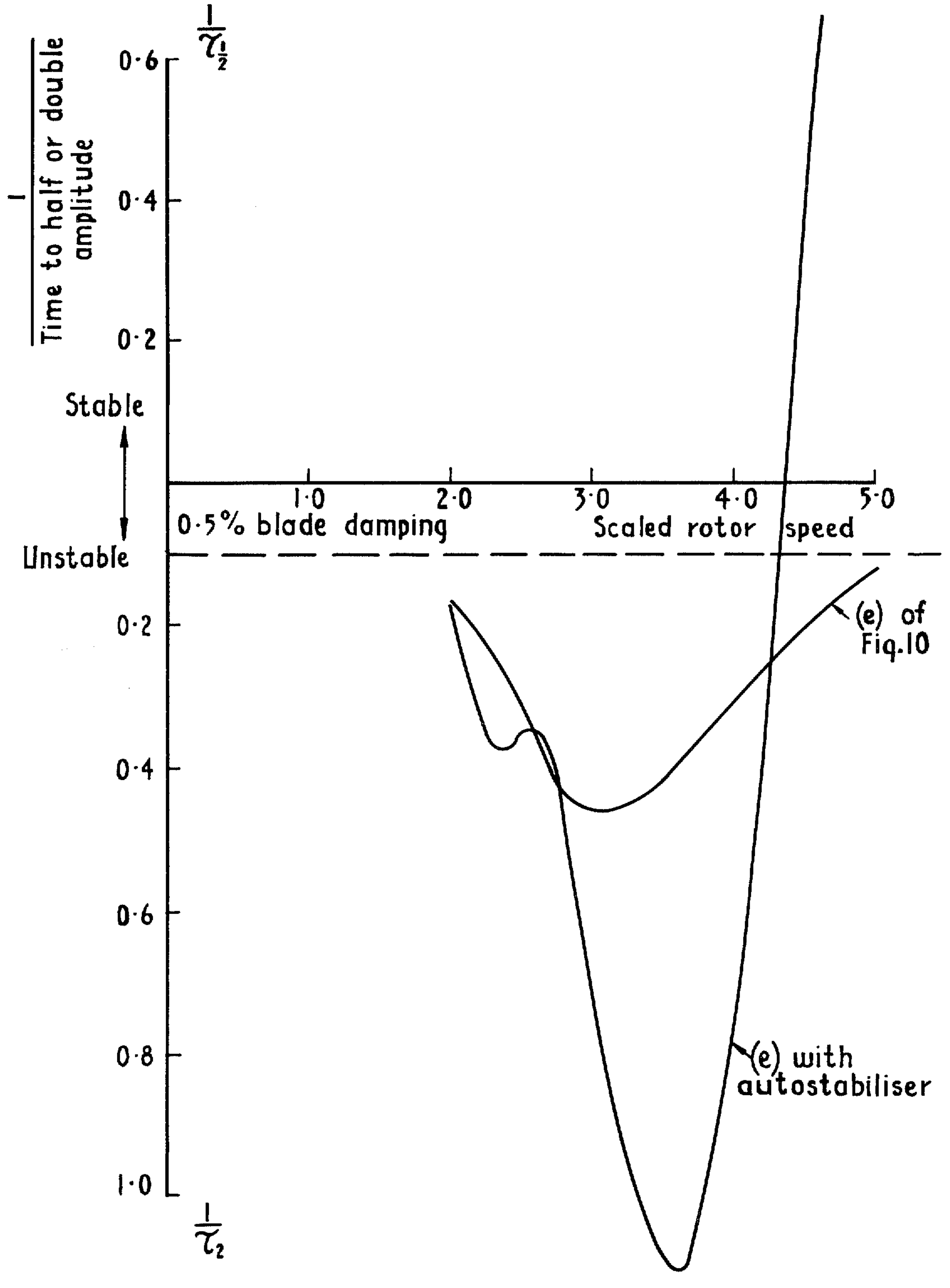

FIG. 14. Variation of lag mode (A) with rotor speed—effect of autostabiliser.

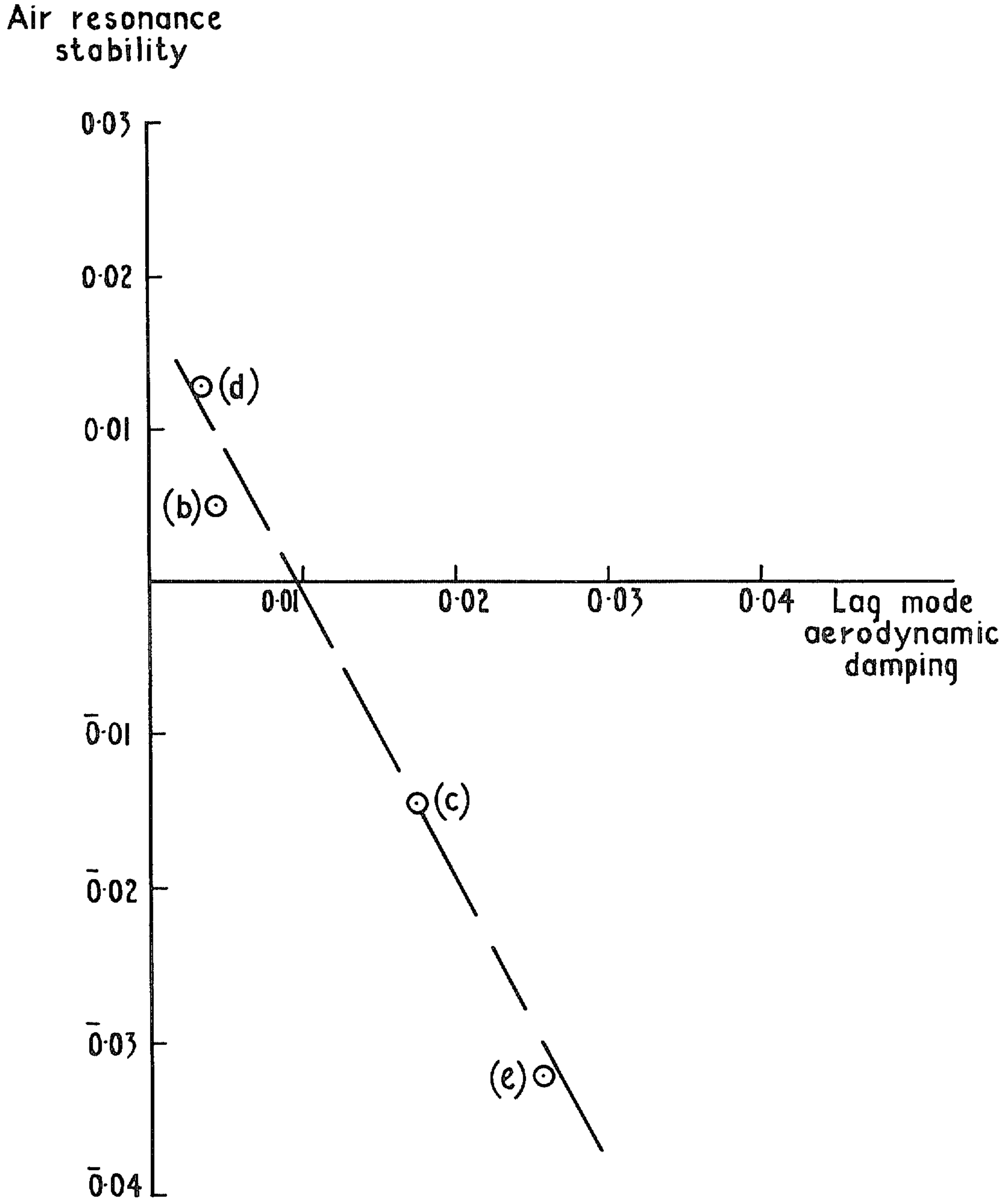

FIG. 15. Correlation of air resonance stability and aerodynamic damping in blade lag mode for cases defined in Section 4.3.

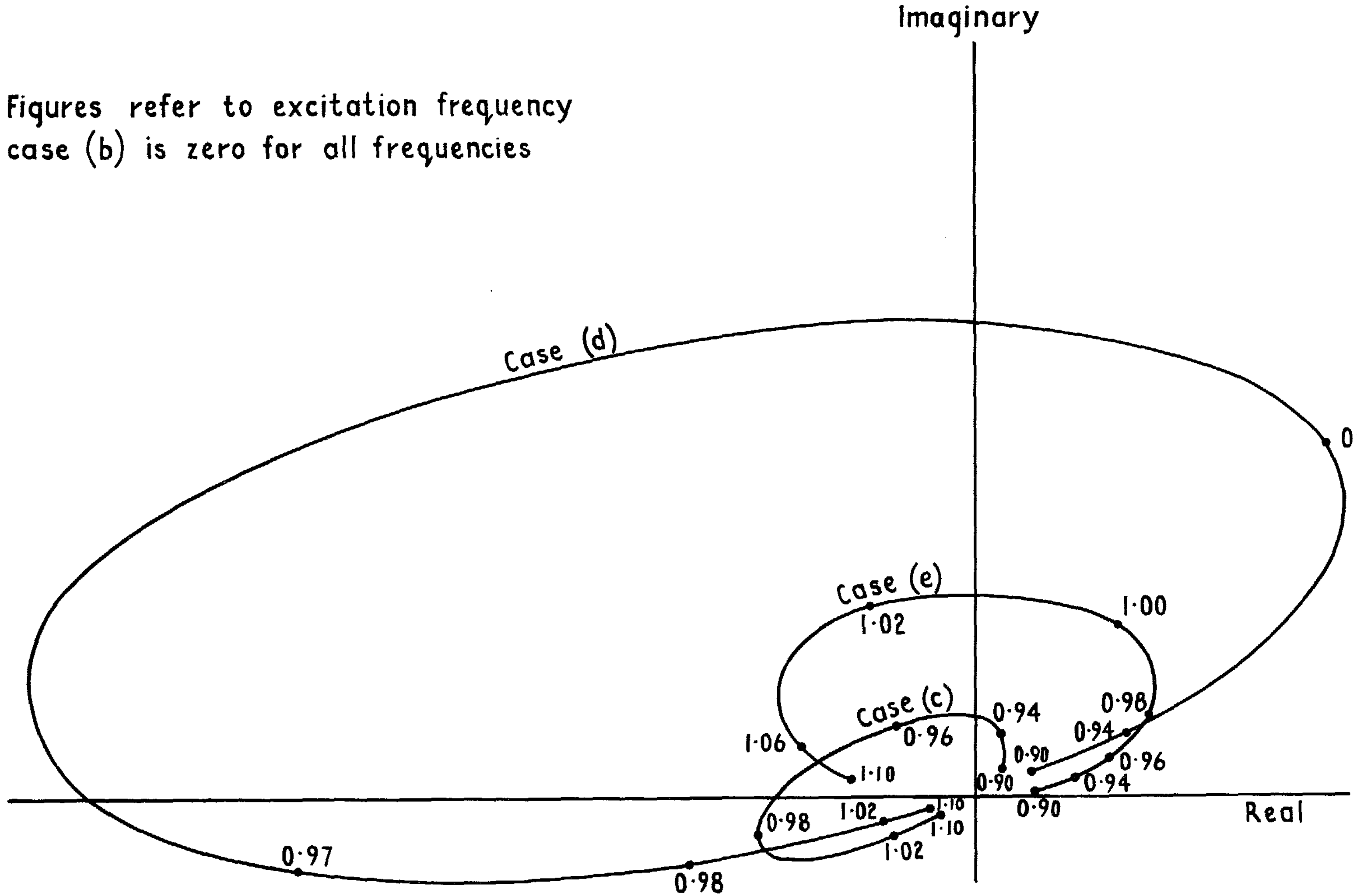

FIG. 16. Impedance of rotor for cases defined in Section 4.3—pitching moment due to fore-and-aft displacement for frequencies close to blade lag mode.

Printed in England for Her Majesty's Stationery Office by J. W. Arrowsmith Ltd., Bristol BS3 2NT
Dd. 505715 K.5. 3/74.

© *Crown copyright* 1974

HER MAJESTY'S STATIONERY OFFICE

Government Bookshops

49 High Holborn, London WC1V 6HB
13a Castle Street, Edinburgh EH2 3AR
41 The Hayes, Cardiff CF1 1JW
Brazennose Street, Manchester M60 8AS
Southey House, Wine Street, Bristol BS1 2BQ
258 Broad Street, Birmingham B1 2HE
80 Chichester Street, Belfast BT1 4JY

Government publications are also available through booksellers

R. & M. No. 3743
ISBN 0 11 470836 3